

Molecular Docking and Dynamics Simulation of Several Flavonoids Predict Cyanidin as an Effective Drug Candidate Against SARS-CoV-2 Spike protein

Asmita Shrestha

Tribhuvan University

Rishab Marahatha

Tribhuvan University

Bishnu Regmi

Florida A&M University College of Pharmacy and Pharmaceutical Sciences

Salik Ram Dahal

Oklahoma State University

Ram Chandra Basnyat

Tribhuvan University

Niranjana Parajuli (✉ niranjana.parajuli@cdc.tu.edu.np)

Tribhuvan University <https://orcid.org/0000-0002-9233-6489>

Research Article

Keywords: In silico, Pharmacokinetics, Molecular docking, MD simulations

Posted Date: June 23rd, 2022

DOI: <https://doi.org/10.21203/rs.3.rs-1750425/v1>

License: © ⓘ This work is licensed under a Creative Commons Attribution 4.0 International License.

[Read Full License](#)

Version of Record: A version of this preprint was published at Advances in Pharmacological and Pharmaceutical Sciences on November 9th, 2022. See the published version at

<https://doi.org/10.1155/2022/3742318>.

Abstract

Background

In silico method has provided a versatile process of developing lead compounds from a large database in a short duration. Spike (S) protein of SARS-CoV-2 is required for viral entry into the host cell, hence inhibiting it prevents the virus from fusing and infecting the host. This study determined the binding interaction of 36 flavonoids against the S protein receptor-binding domain (RBD) of SARS-CoV-2 through molecular docking and molecular dynamics (MD) simulation. In addition, the molecular mechanics generalized Born surface area (MM/GBSA) approach was used to calculate the binding free energy (BFE). Flavonoids were selected based on their *in vitro* assays on SARS-CoV and SARS-CoV-2, respectively.

Results

Our pharmacokinetics study revealed that cyanidin showed good drug-likeness, fulfilled Lipinski's rule of five, and conferred favorable toxicity parameters. MD simulation showed that cyanidin interacts with S protein and altered the conformation and binding free energy suited.

Conclusion

Based on these findings, we have concluded that cyanidin could be a promising drug against the SARS-CoV-2 S protein.

Background

As the COVID-19 pandemic enters its third year, public health officials must assess where we are and how we may break the SARS-CoV-2 devastating grip on the world. The rapid discovery of many safe and effective COVID-19 vaccines has been one of the pandemic's biggest scientific achievements. However, vaccines alone will not be enough to stop the pandemic due to more transmissible new variants, and vaccines are designed to guard against severe suffering and death [1]. New variants due to mutation in SARS-CoV-2 are a subject of concern because the emerging mutants have a potential for enhanced infectivity, competitive fitness, and transmission [2]. There occurs an accumulation of mutations, which drives viral evolution and genome variability, and this enables the virus to escape host immunity and develop drug resistance [3]. Important mutations have appeared in the SARS-CoV-2 S protein that interacts with the host immune system [4]. The reported variant, omicron (B.1.1.529) [5], has a 30 mutation in S protein along with K417N, which was earlier recognized to reduce the effectiveness of a cocktail of therapeutic monoclonal antibodies [6].

The SARS-CoV-2 S protein is a heavily glycosylated homotrimeric transmembrane protein; the S1 subunit contains an RBD that facilitates viral attachment to the host receptor angiotensin-converting enzyme-2

(ACE-2), and the S2 subunit mediates viral entry by mediating host-viral membrane fusion [7]. The biomechanical strength of ACE2-S protein manages viral adherence and access to host cells [8]. Hence, the S protein of SARS-CoV-2, which plays a crucial role in viral attachment and fusion, could be a potential therapeutic target.

Several strategies have been used to develop antiviral drugs for SARS-CoV-2; to date, some drugs are effective against this virus, but only some neutralizing antibodies and remdesivir have been approved by the US FDA [9]. The drug development against SARS-CoV-2 is mainly focused on interrupting the virus's life cycle by blocking its interaction with the host [10] [11]. An increasing number of recent studies have used computational methods for identifying new drug targets or drug repurposing candidates. Nowadays, various natural compounds have been repurposed/tested using computer-aided drug discovery programs [12]; [13]. *In silico* approaches are cost-effective, actionable approaches that can be used to screen several compounds, enabling the discovery of drug combinations and novel drugs.

Flavonoids, an important class of natural products, can affect CoVs at the initial phase of the entrance, replication, and virion release from the host cells [14]. A stable complex between S protein and flavonoids is expected to form due to ortho di-OH hydroxyl groups in the B ring of flavonols [15]. Many flavonoids have been found to block the life cycle of multiple CoV targets (S protein, proteases, TMPRSS2, etc.) through various mechanisms [16] [17]. Flavonoids, therefore, can act as prophylactic, therapeutic, or indirect inhibitors [18]. Flavonoids in this research were chosen based on previously reported *in vitro* assay data (**Table S1**) to assemble cyanidin and other flavonoids as promising drug candidates against SARS-CoV-2.

Flavonoids and their antiviral potential on coronavirus

Flavonoids are natural phytochemicals with antiviral properties which have been discovered to inhibit different targets of SARS-CoV[19] such as interfering with S protein and blocking enzymatic activities of viral proteases 3-chymotrypsin like proteases (3CL^{Pro}), papain-like proteases (PL^{Pro}). Previous research suggests that methylated flavonoids, such as retusin, could be used as an antiviral or adjuvant medication in the treatment of COVID-19[20]. Flavonoids are promising plant-derived chemicals for treating SARS-CoV-2 infection, either through direct antiviral effects or by controlling the host immunological response to viral infection[21]. An *in silico* technique was used to examine and compare several flavonoids known to have anti-inflammatory and antiviral characteristics in an attempt to suppress the spike glycoprotein of SARS-CoV-2, revealing naringin as a potential therapeutic candidate for COVID-19[22]. Based on molecular docking and ADMET analysis, flavonoids such as cyanidin-3-(p-coumaroyl)-rutinoside-5-glucoside, delphinidin-3-O-beta-D-glucoside 5-O-(6-coumaroyl-beta-D-glucoside), albireodelphin, apigenin 7-(6"-malonylglucoside), and (-) maackiain-3-O-glucosyl-6"-O-malonate were demonstrated as potent inhibitors against S protein, 3CL^{pro}, and RdRP of SARS-CoV-2[23]. Similarly, cyanidin and quercetin were found to inhibit the RNA polymerase function and block interaction sites of S protein[24]. A mixture of 11 flavonol glycosides prepared from *S.persica* was studied using a 3CL-

protease inhibition assay, cytotoxicity study, total flavonoid assay, and molecular docking study which was found to inhibit Mpro, S protein fusion onto host cell[25].

Materials And Methods

Preparation and Molecular Modelling of the Target Protein

The X-ray crystal structure of the SARS-CoV-2 RBD of S glycoprotein (PDB ID: 7NX8) with a resolution of 1.95 Å was retrieved from the Protein Data Bank (PDB). The obtained protein was mutated by replacing lysine (K) with asparagine (N) at position 417 through a sequence editor utilizing the protein builder in Molecular Operating Environment (MOE) software (version 2020.0901). The structure was optimized using the MOE protein preparation module by removing water molecules, adding hydrogen atoms, and assigning atomic charges to all protein atoms. Moreover, energy minimization was done using different force field parameters of the MOE preparation module.

Preparation of Ligands

After a comprehensive literature review, the flavonoids were selected based on their antiviral properties against SARS-CoV and SARS-CoV-2, and the structures were accessed from the PubChem database [26] and Chem Spider [27]. Finally, the chosen flavonoids were processed into mol2 file format using open babel, and the energy minimization for molecular docking was done using the MOE software [28]. The structures of the selected 36 natural antiviral flavonoids and their IC₅₀ values against several viruses, including SARS-CoV, SARS-CoV-2, and dengue, are shown in Fig. 1.

Active Site Prediction

MOE Site Finder, which is based on the concept of alpha spheres, was used to determine the amino acid residues involved in the active pocket of the S protein, where the relative positions and accessibility of the receptor atoms were considered [29]. Further, using the site finder, the number and name of the residues of the active site were predicted. Table 1 shows the detected cavities in the S protein region. Figure 2 shows the binding cavity of the S protein, showing a surface map and active site.

Table 1
Active site residues of the S protein using the Site Finder module.

The binding site of S-RBD	Size of polypeptide	Amino acid residues
1	32	Glu 340, Val 341, Ala 344, Thr 345, Arg 346, Phe 347, Ala 348, Asn 354, Arg355, Lys 356, Ser 399
2	20	Phe 342, Asn 343, Ala 344, Thr 345, Ser 371, Ala 372, Ser 373, Phe 374, Trp 436, Leu 441, Arg 509
3	16	Leu 335, Cys 336, Pro 337, Phe 338, Gly 339, Asn 343, Val 362, Ala 363, Asp 364, Tyr 365, Leu 368, Ser 371

Drug-likeness and ADMET Studies

Identification of drug-like characteristics of selected flavonoids was performed using Lipinski's rule of 5 [30] and the swissADME web tool [31]. ADMET (Adsorption, Desorption, Metabolism, Excretion, and Toxicity) studies and toxicity prediction were assessed through the pkCSM web server [32] and ProTox-II [33], respectively.

Molecular Docking and Validation

MOE and GOLD (genetic optimisation for ligand docking) (version 4.0.1) software packages, [34], were used to predict the protein-ligand interactions. The docking analysis was performed on a Microsoft Windows workstation (Intel Core i5-9400 CPU processor and system memory 4GB RAM). A molecular docking study was conducted on selected flavonoids with SARS-CoV-2 S protein that carries K417N mutation. The docking results were validated by extracting the commercial drug and top-scored metabolites from their original binding site and re-docking them into the same position using the GOLD default docking protocol [35]. Further, the lowest energy pose obtained on re-docking and the previous docking positions of the metabolites were superimposed, and its root means square deviation (RMSD) was calculated.

Molecular Dynamics Simulation

The GROMACS tool was used to produce the protein topology file and parameterize the natural flavonoids' ligand topology. MD simulation for 100 ns was performed in GROMACS 5.1.1 using GROMOS 43a1 force field for the protein-ligand system and HSA-ligand to clarify the facts behind the efficiency of this ligand in protein inhibition [36]; [37]. The PRODRG server was used to obtain a required file of ligand [38]. During the initial step of the simulation, a cubic box was generated around the protein-ligand complex and solvated with Simple Point Charge (SPC) at the range of 1.0 nm between the wall of components of the protein complex. Sodium-ion (Na^+) and chloride ion (Cl^-) with the ionic strength of 0.1 M were added to neutralize the solvated system. The system's energy was minimized through 50,000 steps of the steepest descent approach, followed by an equilibrium process using Berendsen thermostat (NVT) ensembles. The integral time phase was two femtoseconds (fs), and the neighbor list was updated for every twentieth step with a cut-off range of 12 Å using the grid option. Periodic boundary conditions (PBC) were used with a constant number of particles in the system, constant pressure, and constant temperature (NPT) simulation criteria. Equilibration of the system at 1 bar pressure for 1 ns was connected using a Parrinello-Rahman Barostat in this simulation [39]. Using trajectories obtained from MD simulations Root Mean Square Deviation (RMSD), Root Mean Square Fluctuation (RMSF), and the radius of gyration (R_g), were analyzed. The average structure of the complex was estimated within the last 10 ns trajectory of MD simulations before the RMSF computation, and then each residue around the ligand was aligned to the average structure. During the simulation, the stability of the C-alpha atoms in amino acids was taken into account. The stability of the MD trajectories was investigated using the backbone RMSD values of atoms about the S protein complex, and the time evolution plot of R_g was computed to estimate the conformational stability of protein-ligand. The RMSF of all the amino acids

around the ligand at 1 nm was determined using the VMD software to investigate the conformational flexibility of the leading active site during the simulation procedure. The MD runs were executed on an AMD processor (32 cores/64 threads) with 128 GB RAM. The visual analysis of RMSD, RMSF, and Rg was done using VMD.

Calculation of Binding Free Energy (BFE)

The prime MM-GBSA [40] of the Schrodinger suite with the OPLS force field is a popular method to calculate the BFE of binding ligands to proteins. This approach is based on docking a ligand and a protein and calculating binding energy using the following equation [41].

$$\Delta G_{\text{bind}} = \Delta E_{\text{MM}} + \Delta G_{\text{Solv}} + \Delta G_{\text{SA}}$$

Where ΔG_{bind} is the BFE of the protein-ligand system, ΔE_{MM} is the difference in the minimized energies between the protein-ligand complex and the sum of the energies of the free protein and ligand. ΔG_{Solv} is the difference in the GBSA solvation energy of the protein-ligand complex and the sum of the solvation energies for the free protein and free ligand. ΔG_{SA} is the difference in surface area energies for the complex and the sum of the surface area energies for the free protein and free ligand. To prioritize the lead inhibitors, the MM-GBSA technique was applied as a rescoring function. To optimize the molecules and choose the best compounds, BFE obtained from prime MM/GBSA calculations was considered, along with the docking scores.

Results

Pharmacokinetic Profiles of Flavonoids

All of the 36 flavonoids chosen have a high absorption rate. And their skin permeability, the volume of distribution at steady-state (VD_{ss}), CNS permeability, and blood-brain barrier (BBB) permeability were investigated because they play a crucial role in determining drug distribution. Among different cytochromes P450 (CYPs) enzymes, the main focus of our study was human cytochrome P450 3A4 (CYP3A4), which was found to be inhibited by flavonoids 1, 2, 4, 6, 10, 11, 16, 19, 23, 26, 28, 32, 33, 34, and 35 indicating that they may be metabolized in the liver shown in **Table S3**. The toxicity of the selected flavonoids was also predicted using ProTox-II, which computes median lethal dose (LD₅₀) values and toxicity classes. **Table S4** displays LD₅₀ values and toxicity classes of 37 flavonoids predicted by using ProTox-II. In regard of acute oral toxicity, flavonoids numbering 1–9, 11, 12, 14, 25, 26, 28, 31, 32, 34, 35, and 36 are found to fall in toxicity class V (2000 < LD₅₀ ≤ 5000), while 17 in VI (LD₅₀ > 5000). The flavonoids 10 and 13 falls in toxicity class III (50 < LD₅₀ ≤ 300), and the remaining belong to toxicity class IV (300 < LD₅₀ ≤ 2000). In this investigation, most of the flavonoids passed Lipinski's criteria, indicating that they are safe to use as drugs. **Table S5** shows the ADME molecular descriptors of the selected flavonoids designed to inhibit SARS-CoV-2 by the SwissADME server. Table 2 shows the five key

physiochemical parameters of the selected 6 flavonoids which are used to test Lipinski's rule of 5 to evaluate drug likeness, and Table 3 shows the ADMET profiles of the selected 6 flavonoids.

Table 2
Physiochemical parameters of the selected 6 flavonoids predicted by using swissADME

Parameters	Mass (< 500)	Hydrogen bond donor (< 5)	Hydrogen bond acceptor (< 10)	LogP (< 5)	Molar Refractivity (40–130)
4'-O-Methyl Diplacol	454.51	4	7	4.32	126.51
Mimulone	408.49	3	5	4.80	118.85
Neobavaisoflavone	322.35	2	4	3.74	95.69
Malvidin	331.30	4	7	0.71	87.13
Cyanidin	287.24	5	6	0.56	76.17
Tomentin E	472.53	4	8	3.24	126.24

Table 3
ADMET profiles of the selected 6 flavonoids predicted by using pkCSM and ProTox-II.

Parameters	Blood-Brain Barrier (BBB)	Human Intestinal Absorption (HIA)	CYP3A4 inhibitor	AMES toxicity	Hepato toxicity	LD ₅₀	Toxicity class
4'-O-Methyl Diplacol	-1.311	76.952	NO	NO	NO	2000	IV
Mimulone	-1.056	90.287	YES	NO	NO	2000	IV
Neobavaisoflavone	-0.09	94.31	YES	NO	NO	2500	V
Malvidin	-1.560	71.558	YES	NO	NO	5000	V
Cyanidin	-1.357	80.203	YES	YES	NO	5000	V
Tomentin E	-1.396	77.239	NO	YES	NO	10000	VI

Molecular Docking Analysis

As indicated earlier, we used the K417N mutant of SARS-CoV-2 S protein in molecular docking analysis. The IC₅₀ values, GOLD Fitness Score, bond length, and RBD interacting residues for the top-scored flavonoids are presented in Table 4. A prior in vitro investigation on SARS-CoV-2 identified cyanidin as a promising treatment candidate, and the current study shows that it has an appropriate Gold Fitness Score of 51.91, indicating its potency as an S protein inhibitor. Furthermore, 4'-O-methyldiplacol, mimulone, neobavaisoflavone, malvidin, and tomentin E also interact appropriately with the binding site of S protein with GOLD Fitness Scores of 63.83, 61.60, 53.90, 52.01, 51.78, and 50.91, respectively. As shown in Fig. 3,

cyanidin interacts with S protein through Asn 343, Ser 371, and Ser 373 via hydrogen bonds and hydrophobic interactions. Similarly, 4'-o-methyldiplacol, mimulone, malvidin, tomentin E, and neobavaisoflavone interact with the protein through different residues documented in the table below. The GOLD Fitness Score, interacting residues of the protein, and interaction distances of all remaining flavonoids studied are displayed in **Table S6**. Similarly, **Figure S1** depicts the 2D and 3D structures of the remaining 4 potential docked protein-ligand complexes.

Table 4
Binding free energies, GOLD Fitness score, interacting residues of proteins, and IC₅₀ values.

Compounds	Binding Free Energies (kcal/mol)	GOLD Fitness Score	Interacting residues of S-RBD	Interaction distance (Å)	IC ₅₀ Value (μM)
Cyanidin	-25.09	51.91	Asn 343	2.26	65.1 ± 14.6 μM (SARS-CoV-2) [42]
			Ser 371	2.37	
			Ser 373	1.96	
			Asn 437	2.97	
			Asn 440	2.2	
Malvidin	-22.03	52.01	Arg 346	2.72	0.04573 μM (SARS-CoV-2) [43]
			Phe 347	1.83	
			Ser 349	2.24	
			Asp 442	2.68	
			Lys 444	2.20	
Tomentin E	-25.02	50.91	Glu 340	2.30	5.0 μM (SARS-CoV) [44]
			Lys 356	2.37	
			Ser 399	2.07	
4'-O-Methyldiplacol	-18.40	63.83	Arg 346	4.07	9.2 μM (SARS-CoV) [44]
			Ala 348	3.57	
			Ser 349	2.35	
			Ser 399	2.43	
Mimulone	-21.23	61.60	Arg 346	2.40	14.4 μM (SARS-CoV) [44]
			Ala 348	3.59	
			Ser 349	2.24	
			Ser 399	2.26	
			Asn 450	2.54	
Neobavaisoflavone	-19.49	53.90	Ser 469	2.72	18.3 μM (SARS-CoV) [45]
			Gln 474	2.54	

Molecular Dynamics Simulation Analysis

MD simulations were run on the docked complex to learn more about the ligand-protein interactions. The RMSD values of the S protein-cyanidin complex and human serum albumin (HSA)-cyanidin complex are shown in Fig. 4 (A). The average RMSD fluctuations for the protein and ligand in the S protein-cyanidin complex is 0.39 nm, with equilibrium after 80 ns. The RMSD of Cyanidin was found to be stable first from 36 to 60 ns and later from 80 ns to 100 ns. Similarly, large deviations in RMSD were observed for the HSA-cyanidin complex, indicating an unstable nature of the complex thus formed. These observations support that cyanidin binds with S protein rather than HSA. The RMSF was measured to further compute the residual flexibility over 100 ns shown in Fig. 4 (B). The RMSF is less than 0.36 nm for each residue surrounding the ligand in the S protein complex, while for HSA, it is 0.5 nm. The Rg trajectory of S protein-cyanidin reaches equilibrium at 35 ns and is steady during 35–100 ns, indicating that the ligand is effectively fitted at the active site of S protein [Figure 4(C)]. In contrast, the Rg trajectory of HSA-cyanidin optimizes equilibrium during 60–80 ns. According to Rg plots, the structural compactness of S protein-ligand remains stable with an average Rg value of 1.6 nm; in contrast, the HSA-cyanidin complex indicates instability with an average Rg value of 3.5 nm. Conclusively, the lower the Rg value higher the compactness of protein-ligand, resulting in a stronger interaction between them [46]; [47].

Binding Free Energies (BFE) Analysis

To quantify the response of active residues with ligands, we performed the prime MM/GBSA method, which calculates the absolute BFE to determine the strength of interaction of the ligand with the protein. The flavonoids cyanidin, mimulone, and 4'-O-methyldiplacol display significantly lower binding energy (ΔG_{bind} -25.09, -21.23, and -18.40 kcal/mol, respectively), indicating that they strongly bind with the protein. BFE calculation revealed the stable binding of cyanidin with S protein, corroborating the molecular docking and conformational dynamics analyses.

Discussions

Despite continued efforts from various research groups, no effective drug against COVID-19 has been developed yet. In search of a safe and effective drug, the computational approach provides a good platform for the virtual screening of metabolites to select the potential drug candidate. Therefore, repurposing natural secondary metabolites could be the most effective way to discover a remedy for COVID-19 infection [48]. To predict the pharmacokinetic properties of potential drugs, ADMET is an important parameter to be considered. For effective metabolism and activity, a good drug candidate should be absorbed in a specific time frame and properly distributed throughout the system. Cytochrome P450s (CYPs) play a key role in phase I of drug biotransformation. Five CYPs (1A2, 2C9, 2C19, 2D6, and 3A4) mediates about 95% of CYP-mediated drug metabolism in the body [49]. ADMET properties of metabolites are analyzed and short-listing of metabolites is done by using the Lipinski rule of five, which determines their drug likeliness property. According to the Lipinski rule, metabolites with a drug-like property should have a molecular weight (mol.wt.) ≤ 500 , hydrogen bond acceptor (HBA) ≤ 10 , and the hydrogen bond donor (HBD) should be ≤ 5 [50]. Due to the structural diversity of flavonoids, it exhibits

versatile biological benefits as anti-inflammatory, neuroprotective, anti-oxidative, as well as antiviral properties [51]. Different specific flavonoids have been reported effective as an antiviral agents for some viruses such as dengue, hepatitis C virus, and influenza by the modification of viral proteins, inhibition of viral entry, and inhibition of viral neuraminidase [52]. The most investigated targets for flavonoid inhibition are proteases (3CLpro and PLpro) of SARS-CoV and MERS-CoV [53]. Flavonoids such as kaempferol are reported to inhibit cation-selective channels formed by the ORF 3a channel of SARS-CoV. As a result, it ultimately inhibits the virus release and stands out as a root of the evolution of new medicinal antiviral drugs [54].

SARS-CoV-2 S-RBD interacts with host receptor angiotensin-converting enzyme (ACE-2) via RBD, laying the groundwork for viral entrance in receptor cells [55]. The emerging variants of SARS-CoV-2 are connected to the mutation on its spike protein, which is important for the entrance of the virus into the host cells [56]. So, our study considered the spike protein as the target protein for molecular docking of flavonoids having an antiviral activity to analyze the GOLD Score and binding interactions of metabolites. The GOLD Score of 4'-o-methyldiplacol, mimulone, and cyanidin was found to be 63.83, 61.60, and 51.91 respectively. But we considered cyanidin as a promising candidate among the above three, as it follows Lipinski's rule of 5 and has been revealed to inhibit the SARS-CoV-2 protein in its derivative form with an IC_{50} value of $65.1 \pm 14.6 \mu\text{M}$ [57]. In addition, cyanidin shows minimum binding energy with the target protein. It is also reported that cyanidin has around 92% inhibition at 150 μM for Mpro enzymatic assay [58]. In our study, cyanidin interacted with S protein forming four hydrogen bonds (with residues Asn 343, Asn 437, Asn 440, and Ser 371) and one pi-alkyl bond (with residue Ala E372); 4'-o-methyldiplacol forms three hydrogen bonds (with residues Ser 399, Ser 349, and Asn 450) and three pi-alkyl bond (with residues Ala 348, Arg 346, and Ala 344); and Mimulone forms three hydrogen bond (with residues Arg 346, Ser 349 and Asn 450) and two pi-alkyl bond (with residues Ala 344, and Ala 348) which may result in its conformational change.

To assess MD trajectories, the RMSD is a crucial calculation. Using the RMSD of a protein-ligand complex system the average distance generated by the dislocation of a given atom over time is calculated [59]. The RMSD of cyanidin was determined to be stable first from 36 to 60 ns and later from 80 ns to 100 ns. The RMSF is used to calculate the flexibility among amino acid residues. It is important for monitoring local protein alterations since it allows you to calculate the average change detected over a large number of atoms to determine the displacement of a given atom relative to the reference structure [60]. The binding pocket was found relatively stable during the MD simulation revealed through obtained RMSF for each residue surrounding the ligand in the S protein complex. Rg reflects the ligand-protein complex compactness, with a smaller radius of gyration indicating a more compact structure [61]. From the calculation of the Rg, cyanidin effectively binds with the spike protein and found that the complex system was suitably stable ranging from 1.675 nm to 1.70 nm. And the MD simulation analysis of the S-protein-cyanidin complex was compared with the HSA-cyanidin complex which reveals the stability of cyanidin complexed with the target protein. It concludes that the cyanidin comes to bind with S protein rather than HSA.

Conclusion

We have used a computational chemistry protocol to identify the most promising flavonoids with in vitro IC_{50} values that inhibit SARS-CoV and SARS-CoV-2 activity. This protocol includes ADMET analysis, molecular docking, molecular dynamics simulations, and BFE calculations to predict whether these flavonoids are suitable for Anti-COVID-19 therapy. This research further enhances that cyanidin interacted with SARS-CoV-2 S protein, exhibiting the best binding poses and forming stable protein-ligand complexes and lower binding free energy. Moreover, 4'-O-methyldiplacol and mimulone also showed promising data, based on molecular docking analysis, but as it falls under toxicity class IV, this study repelled to take them as potent agents. Based on the furnished shreds of evidence, further clinical research of cyanidin and its large-scale clinical trials and mouse model tests is suggested.

Abbreviations

SARS-CoV-2

Severe acute respiratory syndrome coronavirus 2

RBD

Receptor binding domain

MD

Molecular dynamics

MM/GBSA

Molecular-mechanics generalized Born surface area

BFE

Binding free energy

COVID-19

Coronavirus disease 19

ACE-2

Angiotensin-converting enzyme 2

ADMET

Adsorption, distribution, metabolism, excretion, and toxicity

PDB

Protein data bank

MOE

Molecular operating environment

GOLD

Genetic optimisation for ligand docking

RMSD

Root mean square deviation

RMSF

Root mean square fluctuation

Rg
Radius of gyration
HSA
Human serum albumin

Declarations

ETHICS APPROVAL AND CONSENT TO PARTICIPATE

It is not applicable in this research

CONSENT FOR PUBLICATION

Authors agreed to publish this article

AVAILABILITY OF DATA AND MATERIAL

Molecular docking and simulation data generated in this research will be provided upon request to corresponding author.

COMPETING INTERESTS

We declare that there is no conflict of interest regarding the publication of this paper.

FUNDING

This research work is supported by the University Grants Commission (Grants No. CoV-76/77-02), Nepal.

AUTHORS'S CONTRIBUTIONS

Asmita Shrestha and Rishab Marahatha performed computational chemistry work and wrote the manuscript; Bishnu Prasad Regmi and Salik Ram Dahal reviewed the literature and edited the manuscript; Ram Chandra Basnyat and Niranjana Parajuli supervised the research project and edited the draft.

ACKNOWLEDGEMENTS

We are thankful to the University Grants Commission, Nepal.

References

1. M.D. Van Kerkhove, COVID-19 in 2022: controlling the pandemic is within our grasp, *Nat Med.* 27 (2021) 2070–2070. <https://doi.org/10.1038/s41591-021-01616-y>.
2. Y.J. Hou, S. Chiba, P. Halfmann, C. Ehre, M. Kuroda, K.H. Dinnon, S.R. Leist, A. Schäfer, N. Nakajima, K. Takahashi, R.E. Lee, T.M. Mascenik, R. Graham, C.E. Edwards, L.V. Tse, K. Okuda, A.J. Markmann,

- L. Bartelt, A. de Silva, D.M. Margolis, R.C. Boucher, S.H. Randell, T. Suzuki, L.E. Gralinski, Y. Kawaoka, R.S. Baric, SARS-CoV-2 D614G variant exhibits efficient replication ex vivo and transmission in vivo, *Science*. 370 (2020) 1464–1468. <https://doi.org/10.1126/science.abe8499>.
3. M. Pachetti, B. Marini, F. Benedetti, F. Giudici, E. Mauro, P. Storici, C. Masciovecchio, S. Angeletti, M. Ciccozzi, R.C. Gallo, D. Zella, R. Ippodrino, Emerging SARS-CoV-2 mutation hot spots include a novel RNA-dependent-RNA polymerase variant, *J Transl Med*. 18 (2020) 179. <https://doi.org/10.1186/s12967-020-02344-6>.
 4. H. Banoun, Evolution of SARS-CoV-2: Review of Mutations, Role of the Host Immune System, *Nephron*. 145 (2021) 392–403. <https://doi.org/10.1159/000515417>.
 5. D.D. Singh, A. Sharma, H.-J. Lee, D.K. Yadav, SARS-CoV-2: Recent Variants and Clinical Efficacy of Antibody-Based Therapy, *Front. Cell. Infect. Microbiol*. 12 (2022) 839170. <https://doi.org/10.3389/fcimb.2022.839170>.
 6. P. Wang, M.S. Nair, L. Liu, S. Iketani, Y. Luo, Y. Guo, M. Wang, J. Yu, B. Zhang, P.D. Kwong, B.S. Graham, J.R. Mascola, J.Y. Chang, M.T. Yin, M. Sobieszczyk, C.A. Kyratsous, L. Shapiro, Z. Sheng, Y. Huang, D.D. Ho, Antibody resistance of SARS-CoV-2 variants B.1.351 and B.1.1.7, *Nature*. 593 (2021) 130–135. <https://doi.org/10.1038/s41586-021-03398-2>.
 7. S. Pokhrel, B.R. Kraemer, S. Burkholz, D. Mochly-Rosen, Natural variants in SARS-CoV-2 Spike protein pinpoint structural and functional hotspots with implications for prophylaxis and therapeutic strategies, *Sci Rep*. 11 (2021) 13120. <https://doi.org/10.1038/s41598-021-92641-x>.
 8. W. Cao, C. Dong, S. Kim, D. Hou, W. Tai, L. Du, W. Im, X.F. Zhang, Biomechanical characterization of SARS-CoV-2 spike RBD and human ACE2 protein-protein interaction, *Biophysical Journal*. 120 (2021) 1011–1019. <https://doi.org/10.1016/j.bpj.2021.02.007>.
 9. M. Mei, X. Tan, Current Strategies of Antiviral Drug Discovery for COVID-19, *Front. Mol. Biosci*. 8 (2021) 671263. <https://doi.org/10.3389/fmolb.2021.671263>.
 10. S.A. Cherrak, H. Merzouk, N. Mokhtari-Soulimane, Potential bioactive glycosylated flavonoids as SARS-CoV-2 main protease inhibitors: A molecular docking and simulation studies, *PLoS ONE*. 15 (2020) e0240653. <https://doi.org/10.1371/journal.pone.0240653>.
 11. H. Su, Y. Xu, H. Jiang, Drug discovery and development targeting the life cycle of SARS-CoV-2, *Fundamental Research*. 1 (2021) 151–165. <https://doi.org/10.1016/j.fmre.2021.01.013>.
 12. R. Marahatha, S. Basnet, B.R. Bhattarai, P. Budhathoki, B. Aryal, B. Adhikari, G. Lamichhane, D.K. Poudel, N. Parajuli, Potential natural inhibitors of xanthine oxidase and HMG-CoA reductase in cholesterol regulation: in silico analysis, *BMC Complement Med Ther*. 21 (2021) 1. <https://doi.org/10.1186/s12906-020-03162-5>.
 13. R.B. van Breemen, R.N. Muchiri, T.A. Bates, J.B. Weinstein, H.C. Leier, S. Farley, F.G. Tafesse, Cannabinoids Block Cellular Entry of SARS-CoV-2 and the Emerging Variants, *J. Nat. Prod*. 85 (2022) 176–184. <https://doi.org/10.1021/acs.jnatprod.1c00946>.
 14. R. Kaul, P. Paul, S. Kumar, D. Büsselberg, V.D. Dwivedi, A. Chaari, Promising Antiviral Activities of Natural Flavonoids against SARS-CoV-2 Targets: Systematic Review, *IJMS*. 22 (2021) 11069.

- <https://doi.org/10.3390/ijms222011069>.
15. C. Mouffouk, S. Mouffouk, S. Mouffouk, L. Hambaba, H. Haba, Flavonols as potential antiviral drugs targeting SARS-CoV-2 proteases (3CLpro and PLpro), spike protein, RNA-dependent RNA polymerase (RdRp) and angiotensin-converting enzyme II receptor (ACE2), *European Journal of Pharmacology*. 891 (2021) 173759. <https://doi.org/10.1016/j.ejphar.2020.173759>.
 16. M. Russo, S. Moccia, C. Spagnuolo, I. Tedesco, G.L. Russo, Roles of flavonoids against coronavirus infection, *Chemico-Biological Interactions*. 328 (2020) 109211. <https://doi.org/10.1016/j.cbi.2020.109211>.
 17. E.S. Istifli, P.A. Netz, A. Sihoglu Tepe, M.T. Husunet, C. Sarikurkcü, B. Tepe, *In silico* analysis of the interactions of certain flavonoids with the receptor-binding domain of 2019 novel coronavirus and cellular proteases and their pharmacokinetic properties, *Journal of Biomolecular Structure and Dynamics*. (2020) 1–15. <https://doi.org/10.1080/07391102.2020.1840444>.
 18. S. Lalani, C.L. Poh, Flavonoids as Antiviral Agents for Enterovirus A71 (EV-A71), *Viruses*. 12 (2020) 184. <https://doi.org/10.3390/v12020184>.
 19. Y. Yang, M.S. Islam, J. Wang, Y. Li, X. Chen, Traditional Chinese Medicine in the Treatment of Patients Infected with 2019-New Coronavirus (SARS-CoV-2): A Review and Perspective, *Int. J. Biol. Sci.* 16 (2020) 1708–1717. <https://doi.org/10.7150/ijbs.45538>.
 20. C.M. Leal, S.G. Leitão, R. Sausset, S.C. Mendonça, P.H.A. Nascimento, C.F. de Araujo R. Cheohen, M.E.A. Esteves, M. Leal da Silva, T.S. Gondim, M.E.S. Monteiro, A.R. Tucci, N. Fintelman-Rodrigues, M.M. Siqueira, M.D. Miranda, F.N. Costa, R.C. Simas, G.G. Leitão, Flavonoids from *Siparuna cristata* as Potential Inhibitors of SARS-CoV-2 Replication, *Rev. Bras. Farmacogn.* 31 (2021) 658–666. <https://doi.org/10.1007/s43450-021-00162-5>.
 21. M.A. Khazeei Tabari, A. Iranpanah, R. Bahramsoltani, R. Rahimi, Flavonoids as Promising Antiviral Agents against SARS-CoV-2 Infection: A Mechanistic Review, *Molecules*. 26 (2021) 3900. <https://doi.org/10.3390/molecules26133900>.
 22. A.S. Jain, P. Sushma, C. Dharmashekar, M.S. Beelagi, S.K. Prasad, C. Shivamallu, A. Prasad, A. Syed, N. Marraiki, K.S. Prasad, *In silico* evaluation of flavonoids as effective antiviral agents on the spike glycoprotein of SARS-CoV-2, *Saudi Journal of Biological Sciences*. 28 (2021) 1040–1051. <https://doi.org/10.1016/j.sjbs.2020.11.049>.
 23. M.R. Rameshkumar, P. Indu, N. Arunagirinathan, B. Venkatadri, H.A. El-Serehy, A. Ahmad, Computational selection of flavonoid compounds as inhibitors against SARS-CoV-2 main protease, RNA-dependent RNA polymerase and spike proteins: A molecular docking study, *Saudi Journal of Biological Sciences*. 28 (2021) 448–458. <https://doi.org/10.1016/j.sjbs.2020.10.028>.
 24. B.G. Vijayakumar, D. Ramesh, A. Joji, J. Jayachandra prakasan, T. Kannan, *In silico* pharmacokinetic and molecular docking studies of natural flavonoids and synthetic indole chalcones against essential proteins of SARS-CoV-2, *European Journal of Pharmacology*. 886 (2020) 173448. <https://doi.org/10.1016/j.ejphar.2020.173448>.

25. A.I. Owis, M.S. El-Hawary, D. El Amir, H. Refaat, E. Alaaeldin, O.M. Aly, M.A. Elrehany, M.S. Kamel, Flavonoids of *Salvadora persica* L. (meswak) and its liposomal formulation as a potential inhibitor of SARS-CoV-2, RSC Adv. 11 (2021) 13537–13544. <https://doi.org/10.1039/D1RA00142F>.
26. V.D. Hähnke, S. Kim, E.E. Bolton, PubChem chemical structure standardization, J Cheminform. 10 (2018) 36. <https://doi.org/10.1186/s13321-018-0293-8>.
27. H.E. Pence, A. Williams, ChemSpider: An Online Chemical Information Resource, J. Chem. Educ. 87 (2010) 1123–1124. <https://doi.org/10.1021/ed100697w>.
28. I.-J. Chen, N. Foloppe, Drug-like Bioactive Structures and Conformational Coverage with the LigPrep/ConfGen Suite: Comparison to Programs MOE and Catalyst, J. Chem. Inf. Model. 50 (2010) 822–839. <https://doi.org/10.1021/ci100026x>.
29. J. He, D.-Q. Wei, J.-F. Wang, K.-C. Chou, Predicting Protein-Ligand Binding Sites Based on an Improved Geometric Algorithm, PPL. 18 (2011) 997–1001. <https://doi.org/10.2174/092986611796378756>.
30. L.Z. Benet, C.M. Hosey, O. Ursu, T.I. Oprea, BDDCS, the Rule of 5 and drugability, Advanced Drug Delivery Reviews. 101 (2016) 89–98. <https://doi.org/10.1016/j.addr.2016.05.007>.
31. A. Daina, O. Michielin, V. Zoete, SwissADME: a free web tool to evaluate pharmacokinetics, drug-likeness and medicinal chemistry friendliness of small molecules, Sci Rep. 7 (2017) 42717. <https://doi.org/10.1038/srep42717>.
32. D.E.V. Pires, T.L. Blundell, D.B. Ascher, pkCSM: Predicting Small-Molecule Pharmacokinetic and Toxicity Properties Using Graph-Based Signatures, J. Med. Chem. 58 (2015) 4066–4072. <https://doi.org/10.1021/acs.jmedchem.5b00104>.
33. P. Banerjee, A.O. Eckert, A.K. Schrey, R. Preissner, ProTox-II: a webserver for the prediction of toxicity of chemicals, Nucleic Acids Research. 46 (2018) W257–W263. <https://doi.org/10.1093/nar/gky318>.
34. G. Jones, P. Willett, R.C. Glen, A.R. Leach, R. Taylor, Development and validation of a genetic algorithm for flexible docking 1 Edited by F. E. Cohen, Journal of Molecular Biology. 267 (1997) 727–748. <https://doi.org/10.1006/jmbi.1996.0897>.
35. K. Onodera, K. Satou, H. Hirota, Evaluations of Molecular Docking Programs for Virtual Screening, J. Chem. Inf. Model. 47 (2007) 1609–1618. <https://doi.org/10.1021/ci7000378>.
36. P. Mark, L. Nilsson, Structure and Dynamics of the TIP3P, SPC, and SPC/E Water Models at 298 K, J. Phys. Chem. A. 105 (2001) 9954–9960. <https://doi.org/10.1021/jp003020w>.
37. N. Okimoto, N. Futatsugi, H. Fuji, A. Suenaga, G. Morimoto, R. Yanai, Y. Ohno, T. Narumi, M. Taiji, High-Performance Drug Discovery: Computational Screening by Combining Docking and Molecular Dynamics Simulations, PLoS Comput Biol. 5 (2009) e1000528. <https://doi.org/10.1371/journal.pcbi.1000528>.
38. A.W. Schüttelkopf, D.M.F. van Aalten, PRODRG: a tool for high-throughput crystallography of protein–ligand complexes, Acta Crystallogr D Biol Crystallogr. 60 (2004) 1355–1363. <https://doi.org/10.1107/S0907444904011679>.
39. S. Mazumder, S.R. Dahal, B.P. Chaudhary, S. Mohanty, Structure and Function Studies of Asian Corn Borer *Ostrinia furnacalis* Pheromone Binding Protein2, Sci Rep. 8 (2018) 17105.

<https://doi.org/10.1038/s41598-018-35509-x>.

40. C. Mulakala, V.N. Viswanadhan, Could MM-GBSA be accurate enough for calculation of absolute protein/ligand binding free energies?, *Journal of Molecular Graphics and Modelling*. 46 (2013) 41–51. <https://doi.org/10.1016/j.jmglm.2013.09.005>.
41. S.K. Tripathi, S.K. Singh, P. Singh, P. Chellaperumal, K.K. Reddy, C. Selvaraj, Exploring the selectivity of a ligand complex with CDK2/CDK1: a molecular dynamics simulation approach: EXPLORING THE SELECTIVITY OF A LIGAND COMPLEX WITH CDK2 AND CDK1, *J. Mol. Recognit.* 25 (2012) 504–512. <https://doi.org/10.1002/jmr.2216>.
42. E. Pitsillou, J. Liang, C. Karagiannis, K. Ververis, K.K. Darmawan, K. Ng, A. Hung, T.C. Karagiannis, Interaction of small molecules with the SARS-CoV-2 main protease in silico and in vitro validation of potential lead compounds using an enzyme-linked immunosorbent assay, *Computational Biology and Chemistry*. 89 (2020) 107408. <https://doi.org/10.1016/j.compbiolchem.2020.107408>.
43. Y. Wu, S.D. Pegan, D. Crich, E. Desrochers, E.B. Starling, M.C. Hansen, C. Booth, L. Nicole Mullinix, L. Lou, K.Y. Chang, Z.-R. Xie, Polyphenols as alternative treatments of COVID-19, *Computational and Structural Biotechnology Journal*. 19 (2021) 5371–5380. <https://doi.org/10.1016/j.csbj.2021.09.022>.
44. J.K. Cho, M.J. Curtis-Long, K.H. Lee, D.W. Kim, H.W. Ryu, H.J. Yuk, K.H. Park, Geranylated flavonoids displaying SARS-CoV papain-like protease inhibition from the fruits of *Paulownia tomentosa*, *Bioorganic & Medicinal Chemistry*. 21 (2013) 3051–3057. <https://doi.org/10.1016/j.bmc.2013.03.027>.
45. D.W. Kim, K.H. Seo, M.J. Curtis-Long, K.Y. Oh, J.-W. Oh, J.K. Cho, K.H. Lee, K.H. Park, Phenolic phytochemical displaying SARS-CoV papain-like protease inhibition from the seeds of *Psoralea corylifolia*, *Journal of Enzyme Inhibition and Medicinal Chemistry*. 29 (2014) 59–63. <https://doi.org/10.3109/14756366.2012.753591>.
46. D. Bhowmik, R. Nandi, R. Jagadeesan, N. Kumar, A. Prakash, D. Kumar, Identification of potential inhibitors against SARS-CoV-2 by targeting proteins responsible for envelope formation and virion assembly using docking based virtual screening, and pharmacokinetics approaches, *Infection, Genetics and Evolution*. 84 (2020) 104451. <https://doi.org/10.1016/j.meegid.2020.104451>.
47. K.H. Liao, K.-B. Chen, W.-Y. Lee, M.-F. Sun, C.-C. Lee, C.Y.-C. Chen, Ligand-Based and Structure-Based Investigation for Alzheimer's Disease from Traditional Chinese Medicine, *Evidence-Based Complementary and Alternative Medicine*. 2014 (2014) 1–16. <https://doi.org/10.1155/2014/364819>.
48. F.R. Bhuiyan, S. Howlader, T. Raihan, M. Hasan, Plants Metabolites: Possibility of Natural Therapeutics Against the COVID-19 Pandemic, *Front. Med.* 7 (2020) 444. <https://doi.org/10.3389/fmed.2020.00444>.
49. E. Schneider, D.S. Clark, Cytochrome P450 (CYP) enzymes and the development of CYP biosensors, *Biosensors and Bioelectronics*. 39 (2013) 1–13. <https://doi.org/10.1016/j.bios.2012.05.043>.
50. D.M. Teli, M.B. Shah, M.T. Chhabria, In silico Screening of Natural Compounds as Potential Inhibitors of SARS-CoV-2 Main Protease and Spike RBD: Targets for COVID-19, *Frontiers in Molecular*

- Biosciences. 7 (2021) 429. <https://doi.org/10.3389/fmolb.2020.599079>.
51. A.S. Jain, P. Sushma, C. Dharmashekar, M.S. Beelagi, S.K. Prasad, C. Shivamallu, A. Prasad, A. Syed, N. Marraiki, K.S. Prasad, In silico evaluation of flavonoids as effective antiviral agents on the spike glycoprotein of SARS-CoV-2, *Saudi Journal of Biological Sciences*. 28 (2021) 1040–1051. <https://doi.org/10.1016/j.sjbs.2020.11.049>.
52. P. Ninfali, A. Antonelli, M. Magnani, E.S. Scarpa, Antiviral Properties of Flavonoids and Delivery Strategies, *Nutrients*. 12 (2020) 2534. <https://doi.org/10.3390/nu12092534>.
53. R. Kaul, P. Paul, S. Kumar, D. Büsselberg, V.D. Dwivedi, A. Chaari, Promising Antiviral Activities of Natural Flavonoids against SARS-CoV-2 Targets: Systematic Review, *International Journal of Molecular Sciences*. 22 (2021) 11069. <https://doi.org/10.3390/ijms222011069>.
54. S. Schwarz, D. Sauter, K. Wang, R. Zhang, B. Sun, A. Karioti, A. Bilia, T. Efferth, W. Schwarz, Kaempferol Derivatives as Antiviral Drugs against the 3a Channel Protein of Coronavirus, *Planta Med*. 80 (2014) 177–182. <https://doi.org/10.1055/s-0033-1360277>.
55. W. Tai, L. He, X. Zhang, J. Pu, D. Voronin, S. Jiang, Y. Zhou, L. Du, Characterization of the receptor-binding domain (RBD) of 2019 novel coronavirus: implication for development of RBD protein as a viral attachment inhibitor and vaccine, *Cell Mol Immunol*. 17 (2020) 613–620. <https://doi.org/10.1038/s41423-020-0400-4>.
56. P.R.S. Sanches, I. Charlie-Silva, H.L.B. Braz, C. Bittar, M. Freitas Calmon, P. Rahal, E.M. Cilli, Recent advances in SARS-CoV-2 Spike protein and RBD mutations comparison between new variants Alpha (B.1.1.7, United Kingdom), Beta (B.1.351, South Africa), Gamma (P.1, Brazil) and Delta (B.1.617.2, India), *Journal of Virus Eradication*. 7 (2021) 100054. <https://doi.org/10.1016/j.jve.2021.100054>.
57. E. Pitsillou, J. Liang, C. Karagiannis, K. Ververis, K.K. Darmawan, K. Ng, A. Hung, T.C. Karagiannis, Interaction of small molecules with the SARS-CoV-2 main protease in silico and in vitro validation of potential lead compounds using an enzyme-linked immunosorbent assay, *Computational Biology and Chemistry*. 89 (2020) 107408. <https://doi.org/10.1016/j.compbiolchem.2020.107408>.
58. B. Pendyala, A. Patras, C. Dash, Phycobilins as potent food bioactive broad-spectrum inhibitor compounds against Mpro and PLpro of SARS-CoV-2 and other coronaviruses: A preliminary Study, 2020. <https://doi.org/10.1101/2020.11.21.392605>.
59. T.A. Bouback, S. Pokhrel, A. Albeshri, A.M. Aljohani, A. Samad, R. Alam, M.S. Hossen, K. Al-Ghamdi, M.E.K. Talukder, F. Ahammad, I. Qadri, J. Simal-Gandara, Pharmacophore-Based Virtual Screening, Quantum Mechanics Calculations, and Molecular Dynamics Simulation Approaches Identified Potential Natural Antiviral Drug Candidates against MERS-CoV S1-NTD, *Molecules*. 26 (2021) 4961. <https://doi.org/10.3390/molecules26164961>.
60. F. Ahammad, R. Alam, R. Mahmud, S. Akhter, E.K. Talukder, A.M. Tonmoy, S. Fahim, K. Al-Ghamdi, A. Samad, I. Qadri, Pharmacoinformatics and molecular dynamics simulation-based phytochemical screening of neem plant (*Azadiractha indica*) against human cancer by targeting MCM7 protein, *Briefings in Bioinformatics*. 22 (2021) bbab098. <https://doi.org/10.1093/bib/bbab098>.

Figures

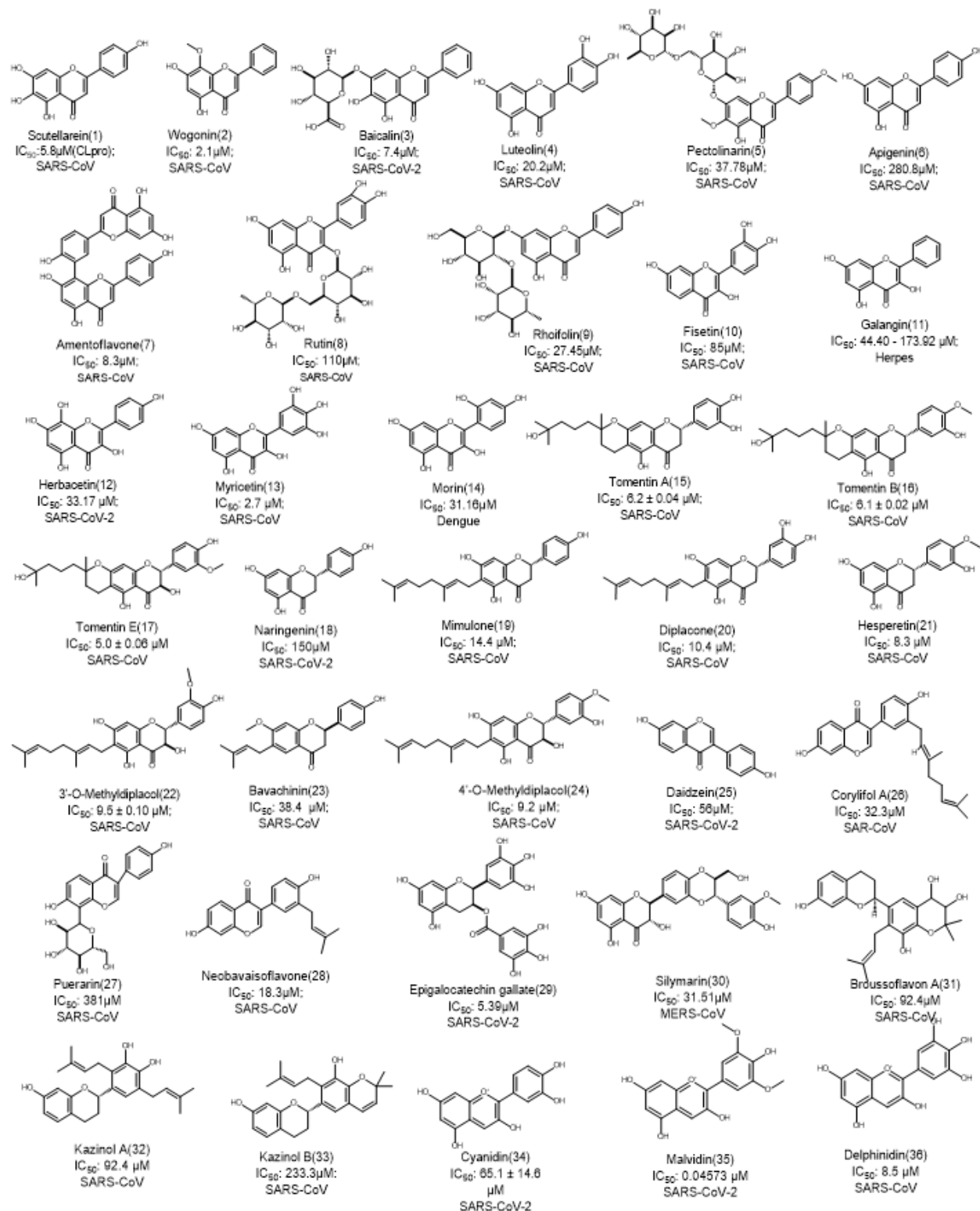


Figure 1

Chemical structures of selected antiviral flavonoids with IC_{50} values against different viruses.

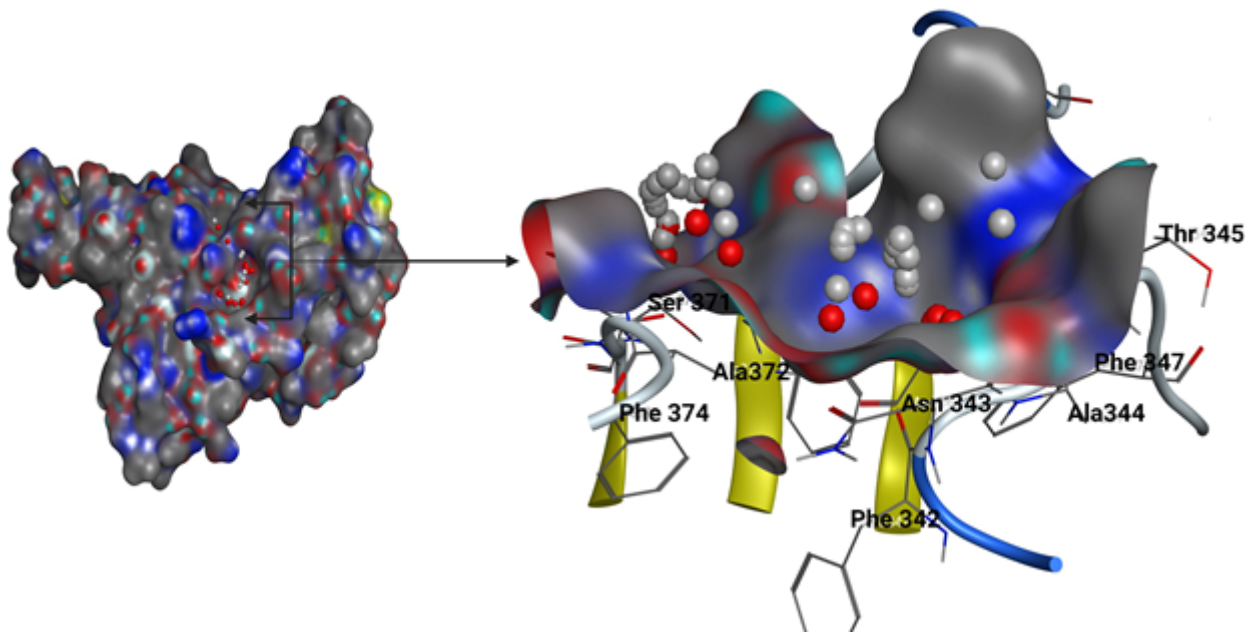


Figure 2

The binding cavity of the S protein shows a surface map (left) and a binding site (right).

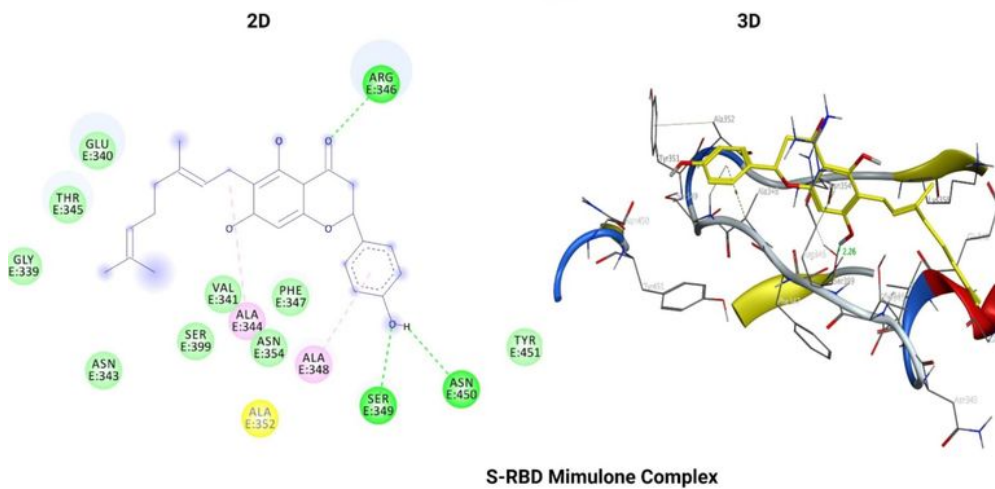
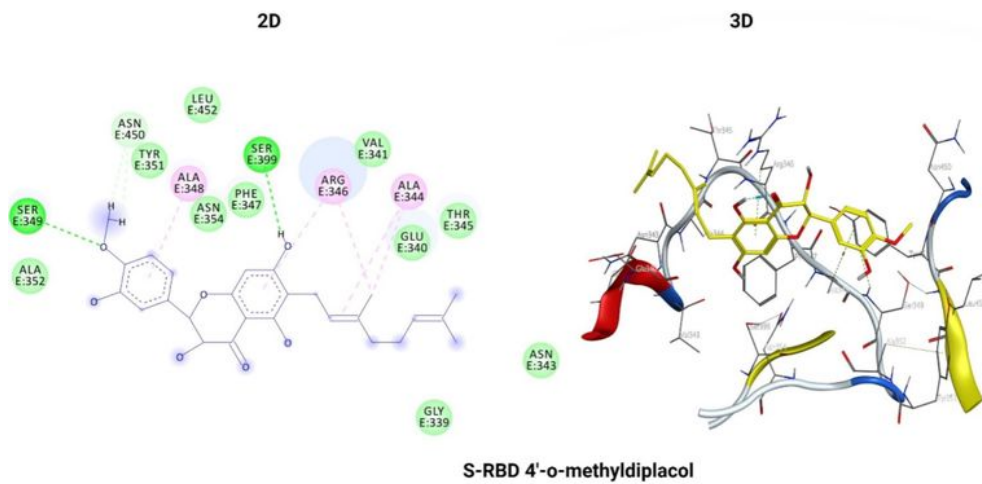
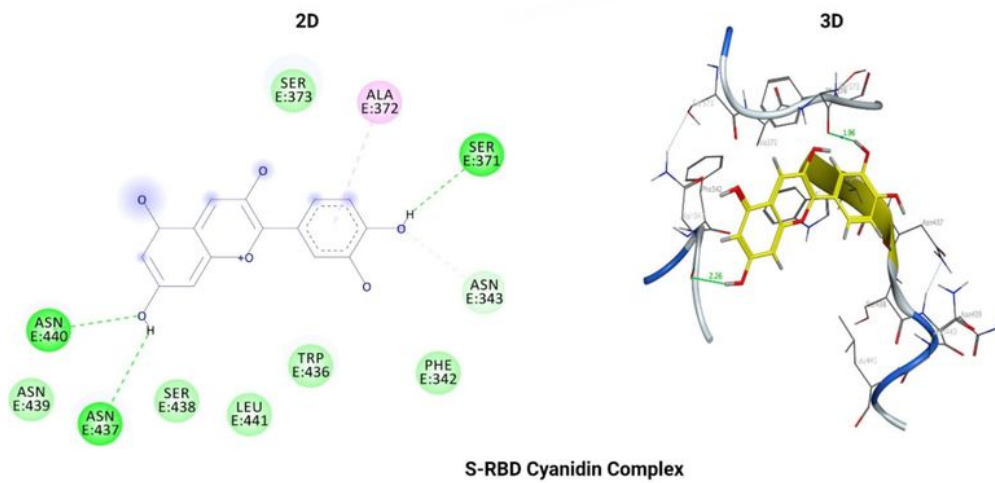


Figure 3

2D and 3D structures of cyanidin, 4'-O-methyldiplacol, and mimulone complexed with SARS-CoV-2 S protein.

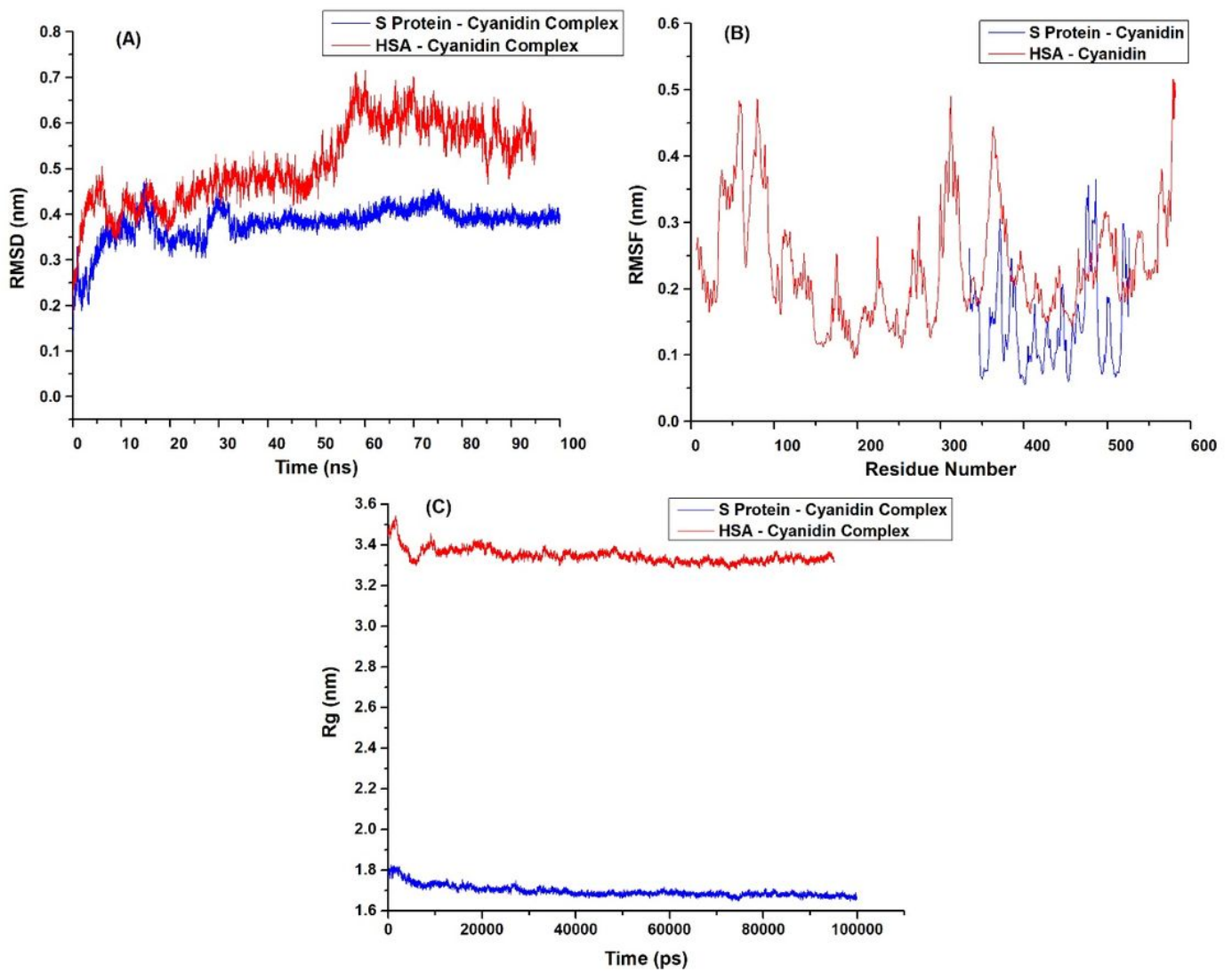


Figure 4

(A) Plot of RMSD, (B) RMSF, and (C) Rg during 100 ns MD simulation of S protein-cyanidin complex and HSA-cyanidin complex.

Supplementary Files

This is a list of supplementary files associated with this preprint. Click to download.

- [GraphicalAbstract.tiff](#)
- [SupplementaryMaterialsFJPS.docx](#)